Lithium-Ion Battery Relaxation Effects

Marvin Messing[1,2], Tina Shoa[2], Saeid Habibi[1]
[1]Department of Mechanical Engineering, McMaster University, Hamilton, ON, Canada,
[2]Cadex Electronics, Richmond, BC, Canada
messingm@mcmaster.ca, habibi@mcmaster.ca, tina.shoa@cadex.com

***Abstract*- The accurate estimation of the state-of-charge (SoC) of lithium-ion batteries is crucial for safely operating electric vehicles. One way to obtain information about SoC is to utilize battery impedance profiles. Effects of temperature, SoC, and state-of-health (SoH) on impedance have been studied using Electrochemical impedance spectroscopy (EIS) but the effect of relaxation period following a charge or discharge cycle requires more attention. In this study EIS results are obtained with respect to relaxation period at different SoCs and temperatures. An impedance model is fit to the data and the change of model parameters with relaxation is analyzed. The results show that the behaviour of the model parameters is in good agreement with electrochemical theory. Furthermore, it is found that changes in some model parameters are significant when compared to changes in SoC. This highlights the need to account for the relaxation effect when measuring battery impedance.**

I. INTRODUCTION

Lithium-ion batteries (LiB) are the current choice for many applications due to their energy density, and long life-span [1]. However, charge and discharge rates, voltage levels, and temperature have to be carefully managed to ensure the safe operation of LiBs [2]. The quality of battery management depends on the accuracy of the estimation of battery states such as state of charge (SoC), and state of health (SoH). These states have to be estimated since they cannot be measured. Instead, battery voltage, current, and temperature are measured, and used in estimation strategies [3]. The most important estimate is the SoC which indicates how much energy is left in the battery. The SoC changes non-linearly as the battery is discharged and depends on the discharge profile. All charge is depleted once the lower voltage limit – which is determined by the manufacturer – is reached. One factor determining the accuracy of SoC estimation is the SoH of the battery. The SoH affects the maximum capacity that the battery can supply at any point in its life, relative to the initial rated capacity. The SoH changes due to aging mechanisms inside the battery [4], which depend on the operating conditions during the lifetime of the battery. Therefore, SoC must be estimated using measurable signals such as voltage, current, and temperature, but also by factoring in how the behaviour of the battery changes as a function of SoH.

The management of LiBs is particularly important for battery packs in electric vehicles (EV). A wide variety of parameter estimation techniques are available for EV applications, collectively covering most operating conditions and individually showing reasonable tracking accuracy [5].

However, the challenge remains to find a more accurate, reliable, universal, and feasible estimation strategy.

Battery states are also related to battery impedance. Battery impedance holds useful information about the internal condition of the battery. Impedance is the combination of reactance and resistance. In batteries, impedance comes from the interaction between different materials, the material characteristics themselves, and chemical reactions [6]. Impedance can be modeled using fundamental electrical circuit components such as resistors and capacitors. However, imperfect circuit elements must be used to increase the modeling accuracy. Models containing such imperfect elements are referred to in this work as impedance models, to distinguish them from ideal equivalent circuit models (ECM).

Electrochemical impedance spectroscopy (EIS) is a method frequently used to characterize the impedance of batteries. In this method, the battery response to a small, sinusoidal signal at multiple frequencies is measured. Using the Fourier transform the time domain response can be converted to frequency domain. From the frequency domain data, a characteristic Nyquist plot can be constructed and used to gain insight into the state of the battery, including its internal resistances, capacities and time constants. To accomplish this, the impedance response of a battery is fit to ECMs or impedance models to mimic electrical systems that result in a similar shape of the Nyquist plot, in response to EIS. Any elements used in ECMs or impedance models must relate to internal characteristics of the battery to be meaningful [7]. Hardware to implement EIS is not usually found on-board battery management systems (BMS) in EVs because of the added cost and complexity of the electronics [8]. However, some recent studies have shown EIS implementations utilizing existing electronics [9], [10]. If hardware barriers can be overcome, EIS could provide valuable measurements that can be used in SoC estimation algorithms. Another concern with EIS is that measurements are dependent on a variety of factors such as SoC, SoH, temperature, and time of measurement with respect to other battery excitation (charge/discharge) – known as relaxation. Therefore, the relationships between these

This research was conducted under a CREATE grant from the Natural Sciences and Engineering Research Council of Canada.

variables and the shape of the Nyquist plot must be studied and understood. Many have studied the impact of SoC, SoH, and temperature [11]–[14], however, few have shown the impact of relaxation. In [15], discharge pulses were used to measure the change in lithium-ion battery impedance with relaxation. They found that many ECM parameters change with relaxation for different SoCs and discharge currents. In [16] the change in OCV with relaxation time was analyzed. Here, time constants of ECM parameters were related to SoH. Relaxation was investigated by [17]–[19]. The relaxation effect was acknowledged by [15] as part of an impedance characterization study and changes in the Nyquist plot were shown to 40 hours. They concluded that impedance changes due to relaxation are small compared to impedance changes due to temperature and SoC but significant enough to require the relaxation effect to be accounted for when comparing impedance results. In [18] the Nyquist plots were shown to stabilize after relaxation of 4 hours under constant SoC and temperature. In [19] relaxation effects were shown to still be visible after 10 hours, and a range of SoCs and temperatures were tested. Both [18] and [19] tested different lithium ion chemistries and battery formats, and developed models to explain the cause of relaxation.

The proposed study aims to provide insight into the variation of EIS in relation to relaxation effects for a range of battery conditions for a state of the art commercial, cylindrical cell. In addition, the impact of relaxation on the parameters of an impedance model is analyzed.

II. Experimental

A custom battery test bench was designed to perform unattended relaxation experiments by integrating a BioLogic SP150 potentiostat with Agilent loads and power supplies (N3306A, N6773A respectively) and a Testequity 1007C thermal chamber. In this study a new Samsung INR21700-48G, 4.8 Ah, cylindrical lithium ion battery was used. The cell was conditioned by 10 full charge discharge cycles. The cell was charged as specified by the manufacture's datasheet starting with a constant current (CC) phase at 0.3C 4.2V followed by a constant voltage (CV) phase to 0.02C cut-off current. Full discharge was done at 0.2C to 2.5 V in CC mode, and SoC targets between 100% and 30% were obtained at 0.2C as well using ampere-hour counting. EIS data was collected between frequencies of 30 mHz to 30 kHz with a voltage amplitude of 5 mV, 6 points per decade and 5 sine wave periods per frequency. EIS data was measured immediately after reaching the target SoC (via discharge only), and re-measured at 30, 60, 180, 300, and 420 minutes. The relaxation test was performed at 25 $°C$ and 40 $°C$ cell surface temperature.

III. Results and Discussion

The EIS response of a battery was measured as described in the previous section to capture the relaxation effect. The relaxation test was repeated three times to ensure the repeatability of the impedance data. It was found that relaxation effects could be distinguished from repeatability errors. The average standard deviation of the impedance was found to be 4.6e-05 $m\Omega$. Fig. 1 shows Nyquist plots for impedance data at 24 $°C$ and 40 $°C$ and how the impedance changes from 100 % to 70 % to 30 % SoC. In the following subsections the impedance data is fit to a model and the change of model parameters with respect to the relaxation effect is analyzed.

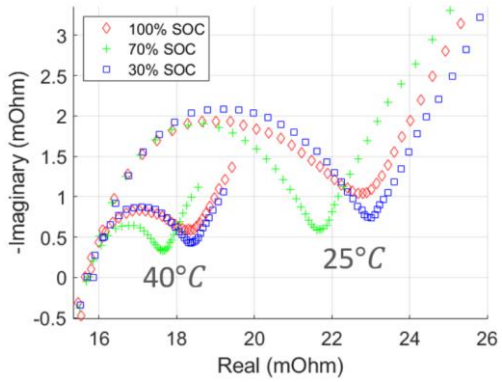

Fig. 1. Nyquist plots for 100%, 70% and 30% SoC at 25$°C$ and 40$°C$.

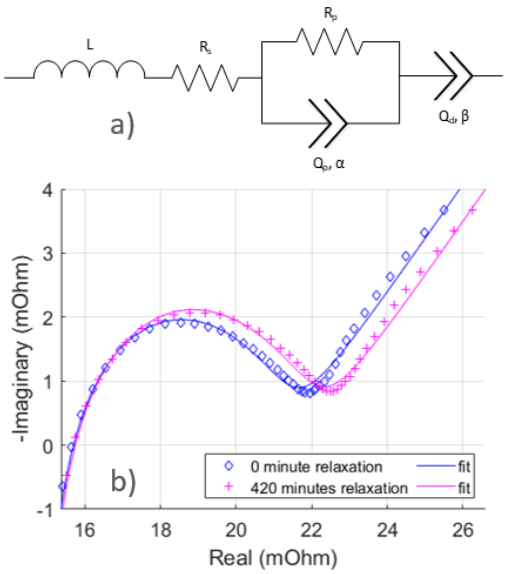

Fig. 2. Impedance model used to model relaxation effect a), and model fit to relaxation data at 25$°C$ and 90% SoC b).

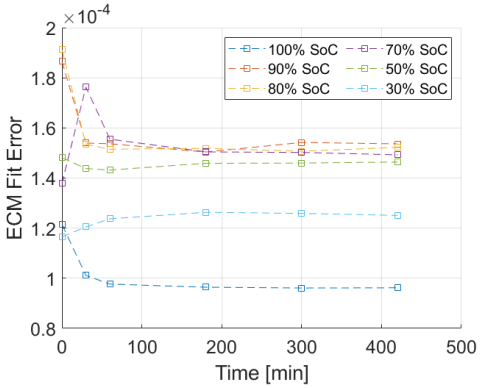

Fig. 3. Impedance model fitting error with different SoCs over different rest times.

A. *Impedance Model*

Fig. 2a shows an ECM adopted from [20] and used in this work. The complex impedance Z of this ECM changes with frequency ω according to (1), where the time constant $\tau = (R_p Q_p)^{1/\alpha}$.

$$Z(\omega) = i\omega L + R_s + R_p/(1+R_p Q_p(i\omega\tau)^{\alpha}) + 1/Q_p(i\omega)^{\beta} \quad (1)$$

Here, i is the applied current magnitude, L is the inductance due to cables used for measurment, and R_s is the ohmic

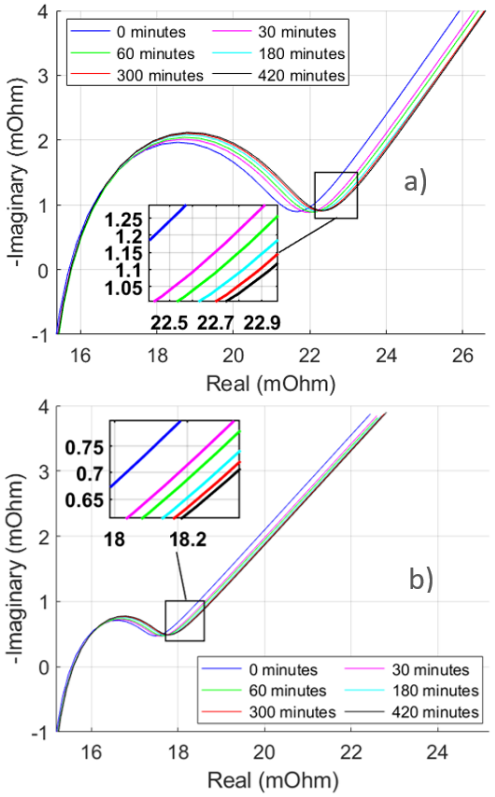

Fig. 4. Modelled relaxation effect at 90% SoC and 25°C a), and 40°C b).

resistance of the battery. R_p and Q_p, α define the polarization resistance and a constant phase element (CPE) for capacitive effects from the electric double layer. Together they form a ZArc element. Finally, Q_d, β defines another CPE to capture the solid-state diffusion process. The impedance model can fit the EIS data well as shown in Fig. 2b for impedance data after discharge to 90% SoC with no rest and 7 hours of rest. The impedance model parameters were optimized using a combination of non-linear least squares and particle swarm optimization algorithms. However, neither algorithm was able to produce fits with consistent fitting error. Fig. 3 shows how the fitting error changes for different SoCs and relaxation times. The model fit has greater error at zero rest and stabilizes to a constant value for data at 60 minutes and after. This fitting error must be considered when analyzing the relaxation results.

Fig. 4 shows how the fit evolves with relaxation time at 25 °C and 40 °C. The change of the Nyquist plot between 5 and 7 hours is small but still present and is smaller at higher temperature when compared to the lower temperature. It can be observed that after 5 hours the change in battery impedance has slowed significantly. However, it is unclear when exactly it has slowed significantly enough such that any further impedance changes are negligible. Changes in impedance may be deemed negligible if the change has minimal impact on the fitting of an impedance model. This is because ultimately the impedance model may be used to further analyze the battery behaviour and, therefore, the accuracy and consistency of the model becomes important.

B. Relaxation Effect

To understand how the parameters of the model shown in Fig. 1a change with relaxation time, the percentage change of each parameter P from its value at 7 hours (420 minutes) P_{420} was calculated using (2). P_t is the value of a model parameter

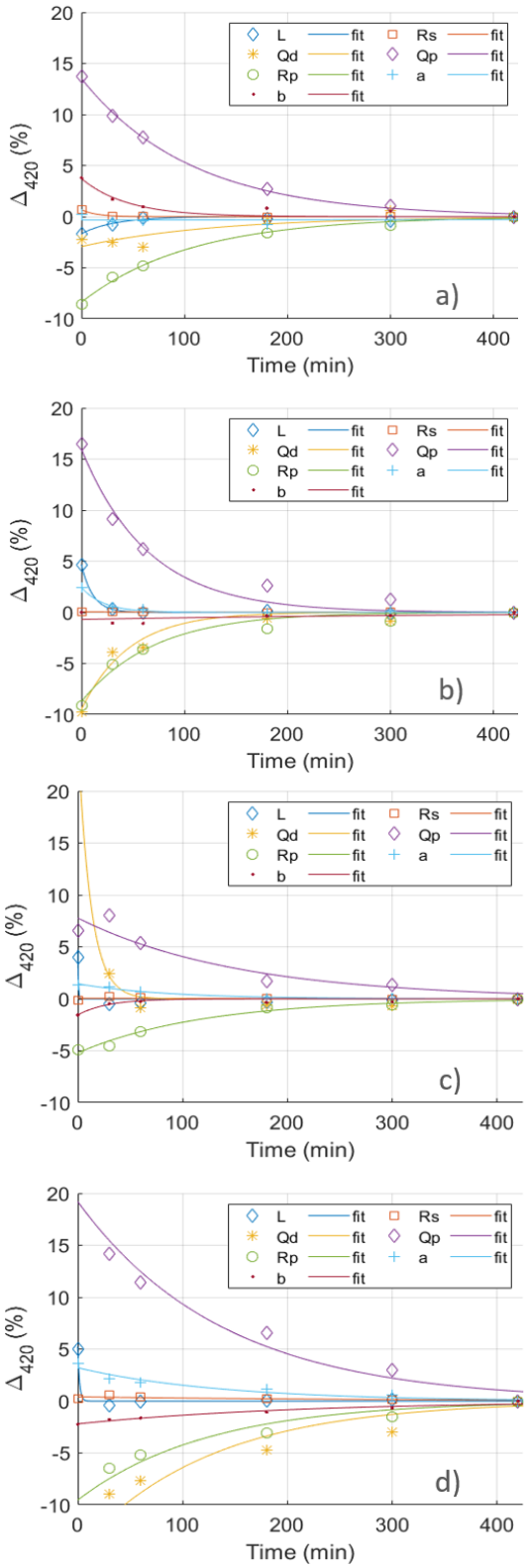

Fig. 5. Percentage change in impedance model parameters from values at 420 minutes at 25°C for a) 100% SoC, b) 90% SoC, c) 70% SoC and d) 30% SoC.

(one of L, R_s, Q_d, Q_p, R_p, a, or b) at relaxation time t. The datasets for each parameter were fit with exponential functions to model the rate of change during relaxation.

$$\Delta_{420} = (P_t - P_{420})/P_{420} \quad (2)$$

Fig. 5 shows Δ_{420} at 25 °C for each model parameter at three SoCs, 100 % a), 90 % b), 70 % c), and 30 % d). The inductance

L and the ohmic resistance R_s stabilize within 10 minutes in all cases. The changes of L and R_s before 10 minutes are inconsonant and likely due to the error introduced by the fitting process as discussed in the previous section. At 100% SoC the parameters with the longest relaxation time are Q_p and R_p, i.e. two components of the ZArc element. The depression constant a (or α) for the first semi-circle does not change. The depression constant for the second semi-circle b (or β) shows a smooth decay at a fast rate. The second CPE parameter Q_d on the other hand shows noisy data points. This may be explained by little or no lithium diffusion at 100% SoC due to low availability of intercalation sites on the anode. At 90% SoC, where more intercalation sites are available and the relatively high cell potential accelerates diffusion, Q_d behaves similar to R_p. At 70 % Q_d stabilizes rapidly again which may indicate a point where the cell potential (driving force) and the SoC (available intercalation sites) work together to equalize concentration gradients [21]. This is reflected by the lower initial values of Δ_{420} for Q_p and R_p. However, while the difference is lower initially, it takes longer for parameters to stabilize due to many available intercalation cites for the lithium and, therefore, potentially longer travel paths [19].

Finally, at 30 % SoC the cell potential is low, such that Q_p, R_p and Q_d equalize slowly despite the large number of available interalation cites. In fact, the relaxation is slowest at 30 % for all three parameters. Lithium slowly diffuses into and through the electrode to find intercalation cites during relaxation. At low SoC this process is slow because of the reduced driving potential. The exponential fit to the Q_p dataset at 30 % SoC (Fig. 5d) suggests that at 420 minutes (7 hours) the cell has not yet stabilized.

At 40 $°C$ (Fig. 6) the model parameters change in a way similar to that at 25 $°C$. The parameters stabilize faster at higher SoC and slower at lower SoC, with 30 % showing the slowest rate of stabilization. The polarization parameters Q_p and R_p stabilize at a slightly slower rate at 40 $°C$ compared with 25 $°C$. This is unexpected because of higher reaction kinetics at higher temperatures. However, the decrease in rate is small, such that additional data will be needed to understand this trend. In contrast, Q_d does stabilize faster in all cases as expected. At 100 % SoC, both diffusion parameters exhibit noisy behaviour again. At 40 $°C$ the exponential fit for Q_p and R_p at 70 % SoC (Fig. 5c) and Q_p at 30 % (Fig. 6d) do not reach steady state, suggesting again that further rest is required.

I. Impedance Maps

Fig. 7 shows how the dominant model parameters Q_p, R_p, and Q_d change with time and SoC at 25 $°C$. The relaxation effect manifests mostly at the edges of the three-dimensional plots. These plots visualize the difference in magnitudes of the parameter change due to relaxation and due to SoC. At the middle range of SoCs (80 % to 40 %) the parameter changes due to relaxation become insignificant when compared to the parameter changes due to SoC. However, the relaxation effect does cause significant parameter changes at the edges of the SoC range (> 90 % and < 40 %). This is evident in Fig. 7 a and c for Q_p and R_p at 25 $°C$. At 40 $°C$ the same can be seen in Fig. 8c for R_p only. The magnitudes of the parameter values also change significantly between 25 $°C$ and 40 $°C$. The diffusion CPE parameter Q_d exhibits a linear trend with SoC from 90 % SoC for both temperatures. This is a useful property of SoC estimation.

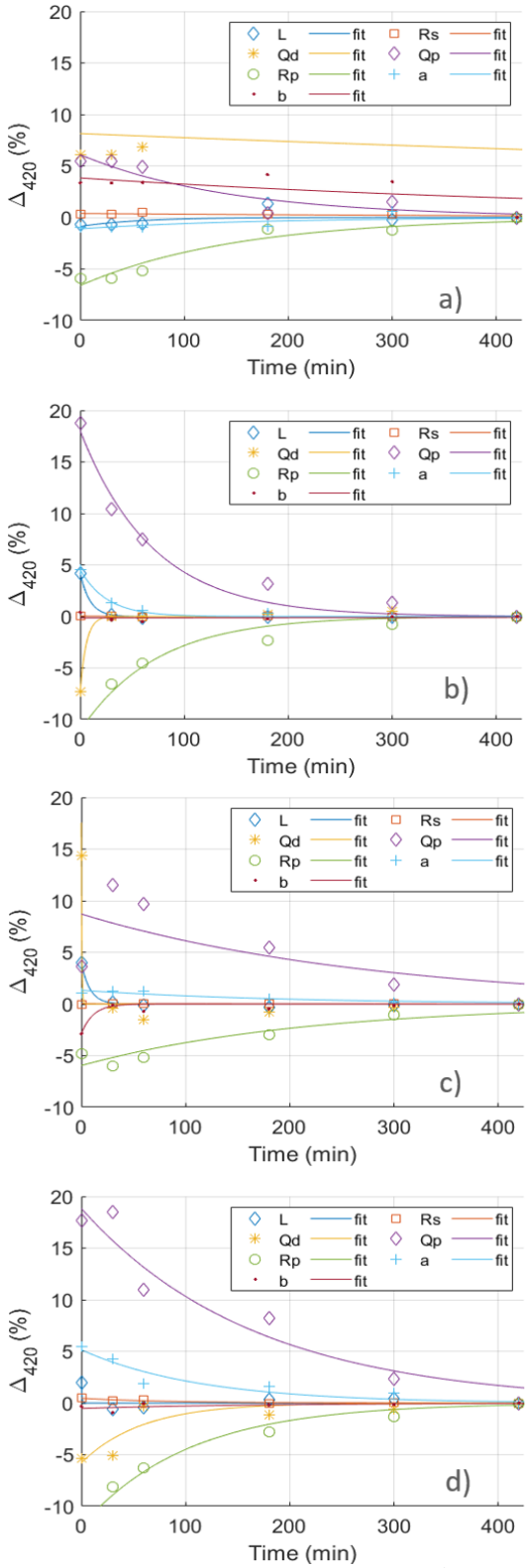

Fig. 6. Percentage change in impedance model parameters from values at 420 minutes at 40°C for a) 100% SoC, b) 90% SoC, c) 70% SoC and d) 30% SoC.

The need for rest time during experiments can be eliminated with the help of impedance maps shown in Fig. 8 and 9, since measurements at 0 minutes can be extrapolated to rest time values. This is especially important for real time applications for EIS measurement where rest times are impractical.

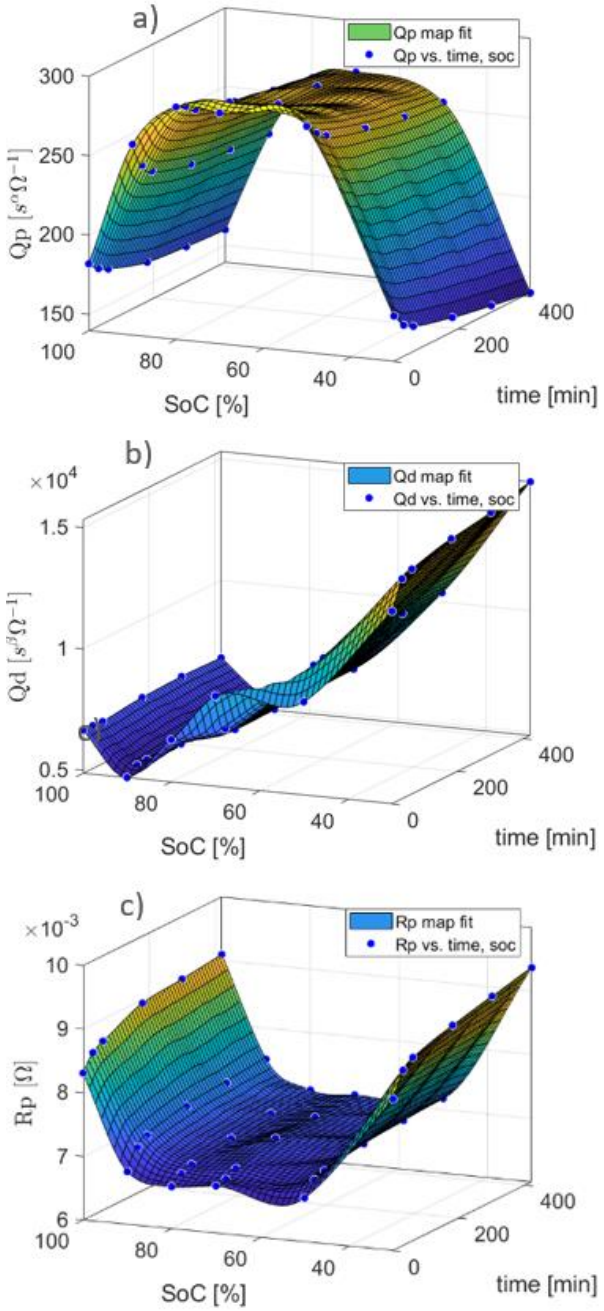

Fig. 7. Impedance maps showing values for a) Qp, b) Qd and c) Rp for different SoCs and rest times at 25°C.

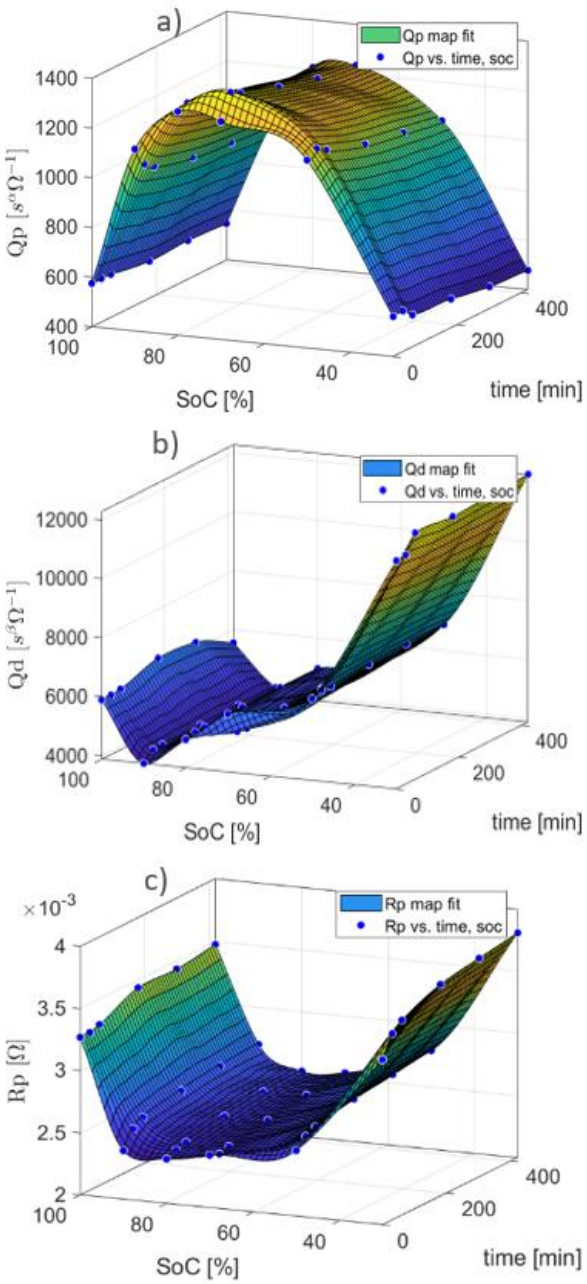

Fig. 8. Impedance maps showing values for Qp, Rp, and Qd for different SoCs and rest times at 25°C (a-c), and 40°C (d-f).

IV. CONCLUSION

In the work presented in this paper the relaxation effect of a commercial lithium ion battery was characterized using EIS and impedance modelling. A suitable impedance model was found in literature and used to model the relaxation effect. The change of each model parameter with relaxation time was analyzed and found to be consistent with electrochemical theory. Results at 40 °C indicate a small decrease in relaxation rate which must be investigated further as it is contrary to previous literature findings. Impedance maps show that the changes in model parameters due to relaxation are significant at certain conditions when compared to the changes in parameters due to SoC and temperature. This should be validated by assessing the impact of the change in model parameters due to relaxation on the accuracy of the model. This work highlights again the need for careful consideration of the relaxation effect. The study will be expanded to longer rest times as well as different temperatures, charge/discharge rates, battery types, and impedance model in future work.

REFERENCES

[1] M. A. Hannan, M. S. H. Lipu, A. Hussain, and A. Mohamed, "A review of lithium-ion battery state of charge estimation and management system in electric vehicle applications: Challenges and recommendations," *Renew. Sustain. Energy Rev.*, vol. 78, no. August 2016, pp. 834–854, 2017.

[2] R. Xiong, J. Cao, Q. Yu, H. He, and F. Sun, "Critical Review on the Battery State of Charge Estimation Methods for Electric Vehicles," *IEEE Access*, vol. 6, pp. 1832–1843, 2018.

[3] L. Ungurean, G. Cârstoiu, M. V Micea, and V. Groza, “Battery state of health estimation : a structured review of models , methods and commercial devices,” no. July 2016, pp. 151–181, 2017.

[4] M. M. Kabir and D. Demirocak, “Degradation mechanisms in Li-ion batteries: a state-of- the-art review,” *Int. J. energy Res.*, vol. 41, no. April 2017, pp. 1963–1986, 2017.

[5] M. U. Cuma and T. Koroglu, “A comprehensive review on estimation strategies used in hybrid and battery electric vehicles,” *Renew. Sustain. Energy Rev.*, vol. 42, pp. 517–531, 2015.

[6] M. Schönleber, C. Uhlmann, P. Braun, A. Weber, and E. Ivers-Tiffée, “A Consistent Derivation of the Impedance of a Lithium-Ion Battery Electrode and its Dependency on the State-of-Charge,” *Electrochim. Acta*, vol. 243, pp. 250–259, 2017.

[7] R. Cottis and S. Turgoose, *Electrochemical Impedance and Noise*. Houston: NACE International, 1999.

[8] J. Meng *et al.*, “An Overview and Comparison of Online Implementable SOC Estimation Methods for Lithium-Ion Battery,” *IEEE Trans. Ind. Appl.*, vol. 54, no. 2, pp. 1583–1591, 2018.

[9] E. Din, C. Schaef, K. Moffat, and J. T. Stauth, “A scalable active battery management system with embedded real-time electrochemical impedance spectroscopy,” *IEEE Trans. Power Electron.*, vol. 32, no. 7, pp. 5688–5698, 2017.

[10] X. Wei, X. Wang, and H. Dai, “Practical on-board measurement of lithium ion battery impedance based on distributed voltage and current sampling,” *Energies*, vol. 11, no. 1, 2018.

[11] P. Kollmeyer, A. Hackl, and A. Emadi, “Li-ion battery model performance for automotive drive cycles with current pulse and EIS parameterization,” *2017 IEEE Transp. Electrif. Conf. Expo, ITEC 2017*, pp. 486–492, 2017.

[12] C. Pastor-Fernández, K. Uddin, G. H. Chouchelamane, W. D. Widanage, and J. Marco, “A Comparison between Electrochemical Impedance Spectroscopy and Incremental Capacity-Differential Voltage as Li-ion Diagnostic Techniques to Identify and Quantify the Effects of Degradation Modes within Battery Management Systems,” *J. Power Sources*, vol. 360, pp. 301–318, 2017.

[13] U. Westerhoff, T. Kroker, K. Kurbach, and M. Kurrat, “Electrochemical impedance spectroscopy based estimation of the state of charge of lithium-ion batteries,” *J. Energy Storage*, vol. 8, pp. 244–256, 2016.

[14] B. Fridholm, T. Wik, and M. Nilsson, “Robust recursive impedance estimation for automotive lithium-ion batteries,” *J. Power Sources*, vol. 304, pp. 33–41, 2016.

[15] H. Wang, M. Tahan, and T. Hu, “Effects of rest time on equivalent circuit model for a li-ion battery,” *Proc. Am. Control Conf.*, vol. 2016–July, pp. 3101–3106, 2016.

[16] P. S. Attidekou, C. Wang, M. Armstrong, S. M. Lambert, and P. A. Christensen, “A New Time Constant Approach to Online Capacity Monitoring and Lifetime Prediction of Lithium Ion Batteries for Electric Vehicles (EV),” *J. Electrochem. Soc.*, vol. 164, no. 9, pp. A1792–A1801, 2017.

[17] W. Waag, S. Käbitz, and D. U. Sauer, “Experimental investigation of the lithium-ion battery impedance characteristic at various conditions and aging states and its influence on the application,” *Appl. Energy*, vol. 102, pp. 885–897, 2013.

[18] A. Barai, G. Chouchelamane, Y. Guo, A. McGordon, and P. Jennings, “A study on the impact of lithium-ion cell relaxation on electrochemical impedance spectroscopy,” *J. Power Sources*, vol. 280, no. Special Issue, pp. 74–80, 2015.

[19] F. M. Kindermann, A. Noel, S. V. Erhard, and A. Jossen, “Long-term equalization effects in Li-ion batteries due to local state of charge inhomogeneities and their impact on impedance measurements,” *Electrochim. Acta*, vol. 185, pp. 107–116, 2015.

[20] J. Schmitt, A. Maheshwari, M. Heck, S. Lux, and M. Vetter, “Impedance change and capacity fade of lithium nickel manganese cobalt oxide-based batteries during calendar aging,” *J. Power Sources*, vol. 353, pp. 183–194, 2017.

[21] T. R. Jow, S. A. Delp, J. L. Allen, J.-P. Jones, and M. C. Smart, “Factors Limiting Li + Charge Transfer Kinetics in Li-Ion Batteries,” *J. Electrochem. Soc.*, vol. 165, no. 2, pp. 361–367, 2018.